Available online at
http://journal.uitm.edu.my/ojs/index.php/BEJ

e-ISSN: 2637-0395

Built Environment Journal 23(2) 2026, 380 – 397.

Built Environment Journal

Evaluating the Accuracy of the Global Digital Elevation Model Using GNSS Levelling

Mohd Faizuddin Abd Rahman[1*], Ami Hassan Md Din[2], Siti Norshahira Mohd Yamen[3]

[1]*Faculty of Asia Built Environment and Surveying, Universiti Geomatika Malaysia, 54200 Kuala Lumpur, Malaysia*
[2]*Geospatial Imaging and Information Research Group (Gi2RG), Faculty of Built Environment and Surveying, Universiti Teknologi Malaysia, 81310 Johor Bahru, Johor, Malaysia*
[3]*Faculty of Built Environment, Universiti Teknologi MARA, 40450 Shah Alam, Selangor, Malaysia*

ARTICLE INFO

Article history:
Received 04 August 2025
Revised 11 November 2025
Accepted 18 January 2026
Online first
Published 01 July 2026

Keywords:
Global Digital Elevation Model
SRTM
ASTER
ALOSW3D
TanDEM-X
GNSS Levelling
Orthometric Height

DOI:
10.24191/bej.v23i2.8382

ABSTRACT

Global Digital Elevation Models (GDEMs) such as Shuttle Radar Topography Mission (SRTM), Advanced Spaceborne Thermal Emission and Reflection Radiometer (ASTER), Advanced Land Observing Satellite World 3D (ALOSW3D), and TerraSAR-X Add-on for Digital Elevation Measurement (TanDEM-X) are widely used for environmental modelling and flood risk assessment. However, their vertical accuracy varies across tropical regions, where terrain, vegetation, and land subsidence complicate elevation measurement. This study evaluates the accuracy of four (4) open-source GDEMs in Peninsular Malaysia using 199 Global Navigation Satellite System (GNSS) levelling benchmarks as reference data. The aim is to determine the best open-source DEM for coastal inundation and flood risk modelling in Peninsular Malaysia. The orthometric heights, H, for the open-source Digital Elevation Model (DEM) were extracted using Global Mapper software and statistically compared in terms of their Root Mean Square Error (RMSE), Correlation Coefficient (R) and Mean Absolute Error (MAE). On the other hand, the orthometric height, H, for the GNSS levelling was derived from the Trimble Business Centre (TBC). Results show that TanDEM-X achieved the highest accuracy (RMSE = 2.480 m, R = 0.900, and MAE = 3.099 m), followed by ALOSW3D, while SRTM and ASTER showed larger deviation between all four (4) GDEMs. The findings highlight TanDEM-X's suitability for coastal inundation and flood risk modelling in Peninsular Malaysia, particularly in low-lying deltaic zones.

[1*] Corresponding author. *E-mail address*: faizuddin@geomatika.edu.my
https://doi.org/10.24191/bej.v23i2.8382

INTRODUCTION

DEM information is widely used in coastal zone management since it provides not only land elevation but also bathymetric information for regions along the shore. Furthermore, the risk assessment for coastal inundation uses DEM to predict rising sea levels and the resulting impact on people's safety along the coastline. The vertical and horizontal precision of DEM plays an important role in examining the danger of coastal inundation since the elevation of the land area typically affects whether a specific zone will be flooded or stay inundated if sea levels rise (Khalid et al., 2016). Nonetheless, the probability of coastal inundation was viewed as significantly higher, particularly in low-lying deltaic land areas (Van De Sande et al., 2012). As a result, these regions are often vulnerable to coastal flooding, necessitating a thorough risk assessment.

DEM datasets can be created using a variety of procedures, including interferometry synthetic aperture radar (IfSAR), radar altimetry, airborne Light Detection and Ranging (LiDAR), and some other traditional surveying techniques such as Global Positioning System (GPS) and levelling (Mukherjee et al., 2012; Athmania and Achour, 2014). In any event, the approaches have both advantages and disadvantages in terms of accuracy, sample density, and pricing. In the context of an aerial approach for producing DEM, LiDAR provides high-precision information and can collect elevation datasets across large areas (Leon et al., 2014). Even though LiDAR generates a very precise DEM, the availability of LiDAR information in specific places may be limited due to the relatively higher cost, in addition to the time required. As a result, many researchers choose to use open-access DEM datasets for analysing the danger of coastal flooding in a specific location (Halim et al., 2019).

The open-access global DEM (GDEM), for example, ASTER, SRTM, ALOS, and TerraSAR-X add-on for daily TanDEM-X, are normally used for assessing the risk of coastal inundation, even though these datasets are slightly lower. However, because its data is publicly available, many scientists are interested in comparing its accuracy using multiple assessment methods. One of the most commonly utilised approaches in assessing the GDEM accuracy is by using GNSS levelling, which involves an in-situ measurement with higher accuracy as ground truthing datum (Gorokhovich & Voustianiouk, 2006; Du et al., 2012). Recent studies across Southeast Asia (El-Ashmawy, 2024; Hussaini et al., 2024; Kumar & Jha, 2023) emphasise that even small vertical errors (< 1 m) in DEMs can lead to substantial misclassification of flood-prone areas. In Malaysia, coastal subsidence, monsoon-driven flooding, and rapid land reclamation further complicate DEM accuracy validation. Thus, a region-specific assessment of open-source GDEMs is necessary to guide coastal modelling and environmental planning.

Therefore, this study aims to assess the accuracy of the four (4) GDEM (ASTER, ALOSW3D, SRTM, and TanDEM-X) by comparing their elevation with GNSS levelling. Among the objectives of this study are (i) to extract the orthometric height, H, from the GDEM USIGN Global Mapper, (ii) to derive the orthometric height, H, from GNSS levelling as ground-truthing data using the GNSS Fast-Static observation technique, and (iii) to assess the accuracy of the GDEM with GNSS levelling in terms of their Orthometric height, H. The statistical assessment involves the Root Mean Square Error (RMSE) and correlation coefficient, R. Theoretically, the GDEM with the smallest RMSE and MAE, and largest correlation coefficient, R, signifies the GDEM with the best accuracy for any topographic application.

https://doi.org/10.24191/bej.v23i2.8382

RESEARCH SCOPE

The following are the research scope for this study.

Study Area

The study region encompasses the area along the east and west coasts of Peninsular Malaysia, as shown in Figure 1. It covers an area of latitude 1° N to 9° N and a longitude of 99° E to 105° E. The west coast features extensive mangrove swamps, reclaimed industrial zones, and deltaic plains (e.g., Klang and Perak estuaries), while the east coast comprises sandy beaches and gently undulating terrain (e.g., Kelantan and Terengganu coasts). These contrasting landforms influence DEM accuracy through differing vegetation density and terrain roughness.

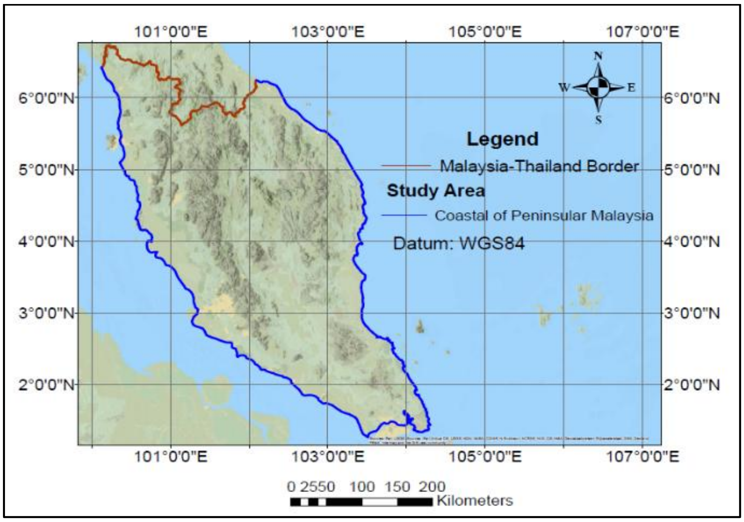

Fig. 1. Study Area Along the Coast of Peninsular Malaysia

Source: Authors (2025)

Global Digital Elevation Model (GDEM) Datasets

The four (4) GDEM datasets assessed in this study comprise SRTM (https://srtm.csi.cgiar.org/), ASTER (http://gdex.cr.usgs.gov/gdex/), ALOSW3D (https://www.eorc.jaxa.jp/ALOS/en/aw3d30/), and TerraSAR-X add-on for daily TanDEM-X (https://download.geoservice.dlr.de/TDM90/). The GDEM data utilised in this study are acquired from an open-source server, and encompass different accuracies and methods, as shown in Table 1. The reason behind the selection of only four (4) GDEMs for this study is due to their data availability and ease of access.

Table 1. List of GDEM and Geoid Models Used in This Study

	ASTER	SRTM30/90	ALOSW3D	TanDEM-X
Data Source	ASTER	Space Shuttle Radar	PRISM	InSAR
Data Provider	METI /NASA	NASA/ CGIAR-CSI	JAXA	DLR and AIRBUS

https://doi.org/10.24191/bej.v23i2.8382

Year of Release	2009	2003	2015	2010
Period of Data Acquisition	2009 - Ongoing	11 Days (in 2000)	2015 - Ongoing	2005 – Ongoing
Spatial Resolution	15 m VIR 30 m SWI 90 m TIR	1-arc second (30 m) 3-arc second (90 m)	1-arc second (30 m)	0.4 arc second (12 m) 1-arc second (30 m) 3-arc second (90 m)
DEM Vertical Accuracy	±20 m	±10 to ±16 m	±30 m	±10 m
Global Coverage of DEM	83 North to 83 South	60 North to 56 South	60 North to 60 South	90 North to 90 South
Vertical Datum	EGM1996	EGM1996	EGM1996	WGS84
Horizontal Datum	WGS84	WGS84	WGS84	WGS84

Source: Authors (2025)

GNSS Levelling

GNSS leveling data were collected along both the east and west coasts of Peninsular Malaysia using fast-static and Network Real-Time Kinematic (NRTK) methods at each observation point, employing a Topcon GR5 receiver, as shown in Figure 2. A total of 199 observations were carried out, with most measurements taken at either Standard Benchmarks (SBM) or Benchmarks (BM), typically located around 10 kilometers inland from the coastline.

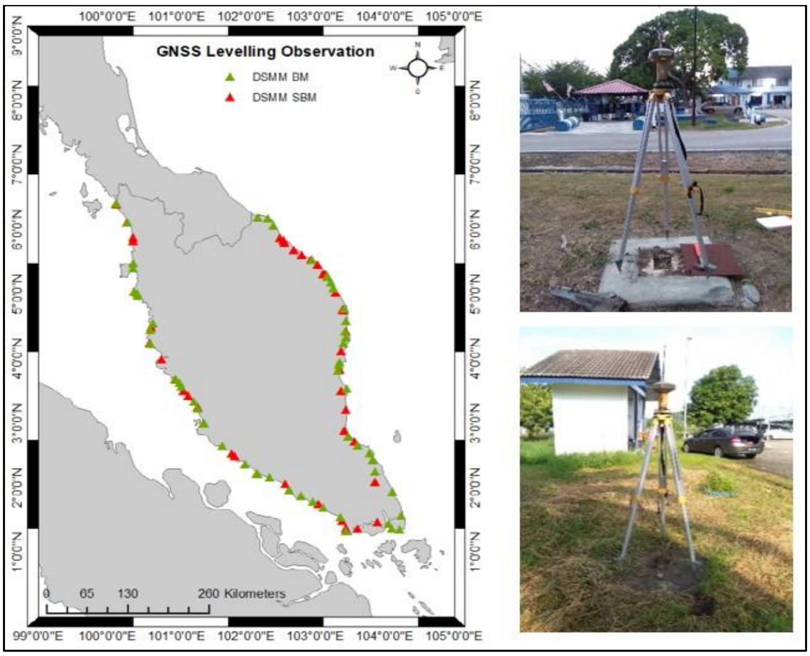

Fig. 2. GNSS Observations on Coastal SBM and BM Using Fast-Static and NRTK Methods

Source: Authors (2025)

Next, the GNSS levelling data were processed using Trimble Business Centre (TBC) software using a single-baseline processing technique with the nearest Virtual Reference Station (VRS) or Malaysia Real-Time Kinematic Network (MyRTKnet) as a base station to obtain the corrected latitude, longitude, and ellipsoidal height, *h*. The derived ellipsoidal height, h, along with the geoid height, N, from Malaysia Precise Gravimetric Geoid (MyGEOID), was then utilised to determine the orthometric height, H, for all 199 GNSS levelling points.

Reference Surface

The reference surface used in this study is the Malaysia Precise Gravimetric Geoid (MyGEOID) and Earth Gravitational Model 1996 (EGM1996). Both reference surfaces are necessary for the conversion of the extracted elevation of the GDEM from Global Mapper to orthometric height, H, with respect to MyGEOID. Making it compatible for comparison with the orthometric height, H, from GNSS levelling.

Relationship between Geoid, Ellipsoid and Topography

A geoid is a possible gravitational field surface that could be thought of as representing the worldwide Mean Sea Level (MSL). As a result, the geoid and MSL can be used for height reference similarly. The MSL figure is the mean of the highest and lowest tide levels recorded at the tide gauge sites over a period of about 18.6 years. It was used as a reference to the height of detail on, above, or below the topography (DSMM, 2005). The height that refers to the geoid of a point above the topographic surface is known as orthometric height, H, while the height that refers to the surface of the ellipsoid is known as ellipsoid height, h. The separation distance between the surface of the ellipsoid and the geoid is known as geoid height, N (DSMM, 2005). The relationship between topography, ellipsoid, and geoid surface is illustrated in Figure 3 (Albayrak et al., 2020).

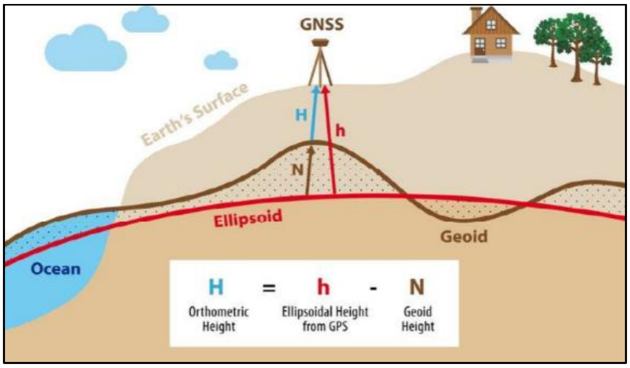

Fig. 3. Relationship between Topography, Ellipsoid, and Geoid

Source: Albayrak et al. (2020)

Malaysia Geoid (MyGEOID)

MyGEOID contains the geoid height value (or N value) relative to the Geodetic Reference System 1980 (GRS80) ellipsoid in grid form (Nordin et al., 2005). It consists of two (2) geoid models, which are West Malaysia Geoid 2004 (WMGEOID04) for Peninsular Malaysia and East Malaysia Geoid 2005 (EMGEOID05) for Sabah and Sarawak (Nordin et al., 2005; Fazilah, 2006). Its establishment was based on airborne and terrestrial gravity measurement, satellite altimeter, global geoid model, and digital terrain model (DTM). In addition, the GPS observation above the level mark has been adjusted to model the vertical datum bias (VDB) in establishing a fitted geoid with its vertical datum based on the MSL (Nordin et al., 2005; Fazilah, 2006).

Earth Gravitational Model 1996 (EGM1996)

The Earth Gravitational Model 1996 (EGM1996) represents Earth's gravitational potential using spherical harmonic coefficients, developed through a joint effort by NASA's Goddard Space Flight Centre, the National Imagery and Mapping Agency (NIMA), and Ohio State University. The model provides a complete set of spherical harmonics up to degree and order 360 (Lemoine et al., 1998). Its construction integrated global gravity observations—including satellite-derived gravity anomalies from ERS-1 and GEOSAT—together with extensive satellite tracking datasets such as GNSS, TDRSS, DORIS, TRANET, and satellite altimetry from TOPEX/Poseidon, ERS-1, and GEOSAT. The EGM1996 model reflects the regional and global character of the Earth's gravity field and not locally (Lemoine et al., 1998). The illustration of MyGEOID and EGM1996 for Peninsular Malaysia is illustrated in Figure 4.

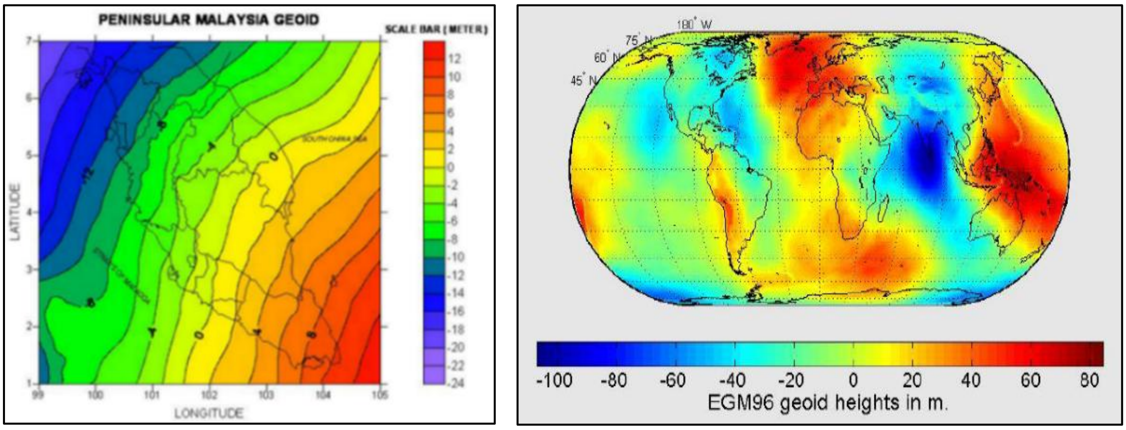

Fig. 4. (left) MyGEOID model for Peninsular Malaysia; (right) EGM1996 GEOID Model

Source: (left) Nordin et al., (2005); Ismail et al. (2018); (right) Rao et al. (2012)

Extraction of Orthometric Height of GDEM from Global Mapper

The process of uploading the GDEM and GNSS levelling coordinates for the determination of the orthometric height, *H*, of 199 GNSS observation points along the east and west coasts of Peninsular Malaysia using Global Mapper is illustrated in Figure 5. This study uses Global Mapper due to its reliability for terrain, slope and elevation analysis, which were the primary aims of this study. Global Mapper allows interpolation and point-based data extraction from the interpolated elevation surface.

https://doi.org/10.24191/bej.v23i2.8382

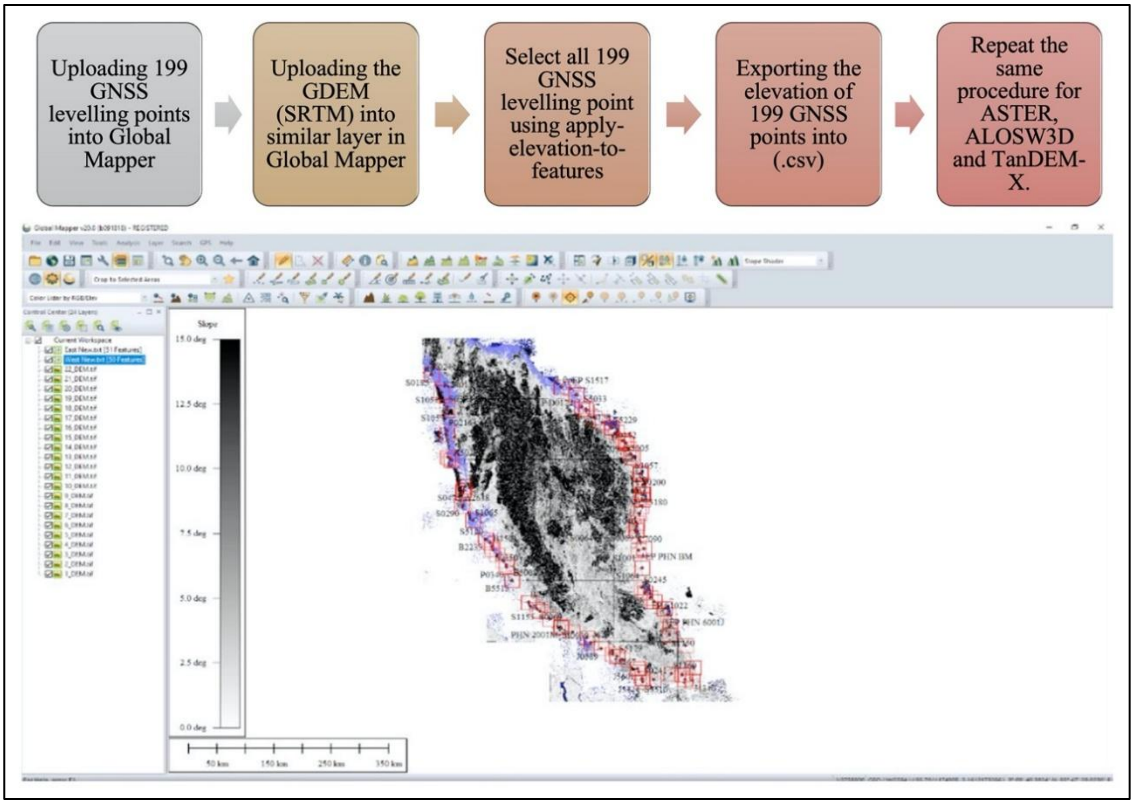

Fig. 5. Extraction of Orthometric Height, *H*, for The Open-Source DEM Using Global Mapper

Source: Authors (2025)

Method of Assessment

There are three (3) statistical assessments utilised in this study for determining the accuracy of the GDEM with GNSS levelling, namely the RMSE, R and MAE.

Root Mean Square Error (RMSE)

The RMSE is an assessment to indicate how dispersed the residual area is, revealing how tightly the observed data cluster around the predicted values. It also illustrates the average difference between a statistical model of the predicted values and the actual values (Chai & Draxler, 2014). Theoretically, the lower the RMSE, the better a given model can fit a dataset. Generally, RMSE indicates how concentrated the data is around the line of best fit (Glen, 2020a). The residual is estimated by subtracting the observed value from the known value, as shown in Equation 1 (Chai & Draxler, 2014).

$$RMSE = \sqrt{\frac{\sum_{i=1}^{N} (Predicted_i - Actual_i)^2}{N}} \quad (1)$$

where,

$Predicted_i$: The predicted value for the i th observation.

$Actual_i$: The observed (actual) value for the i th observation

N: Total number of observations.

Correlation Coefficient, R

In statistical terms, correlation refers to the relationship between two (2) variables in quantitative research and can take on various forms. It comprises the Pearson correlation, Kendall rank correlation, Spearman correlation, and Biserial Point correlation (Glen, 2020b). Correlation measures the degree of association between data variables. Through correlation analysis, it can be determined that changes in one (1) variable are likely to be accompanied by changes in another related variable. In simpler terms, it is a statistical evaluation method used to study the strength of the relationship between two (2) continuous variables measured numerically as shown in Equation 2 (Gogtay & Thatte, 2017).

$$r = \frac{\sum(x_i - \bar{x})(y_i - \bar{y})}{\sqrt{\sum(x_i - \bar{x})^2 \sum(y_i - \bar{y})^2}} \quad (2)$$

where,
x_i : correlation coefficient
$\bar{x}$: values of the x-variable in a sample
y_i : values of the y-variable in a sample
$\bar{y}$: mean of the values of the y-variable

Mean Absolute Error (MAE)

MAE is the average of the absolute differences between the actual value and the predicted value. It is a simple way to quantify how accurate a model is that is less affected by outliers. MAE shows how large the average difference is between predicted (or modelled) values and observed (true) values, regardless of whether the difference is positive or negative, as shown in Equation 3.

$$MAE = \frac{1}{n} \sum_{i=1}^{n} [y_i - \hat{y}_i] \quad (3)$$

where:

y_i= observed (true) value
$\hat{y}_i$= predicted/model value
n= number of samples

DATA EXTRACTION FOR GEOID HEIGHT, N AND ORTHOMETRIC HEIGHT, H

Extraction of Geoid Height, N for MyGEOID and EGM1996

This research employed two (2) geoid models, MyGEOID and the Earth Gravitational Model 1996 (EGM1996). A continuous geoid surface was produced for both models through Inverse Distance

Weighting (IDW) interpolation, enabling the extraction of geoid height (N) values. These geoid height datasets for MyGEOID and EGM1996 were subsequently derived using ArcGIS software. The resulting interpolated geoid surfaces for both models are presented in Figure 6.

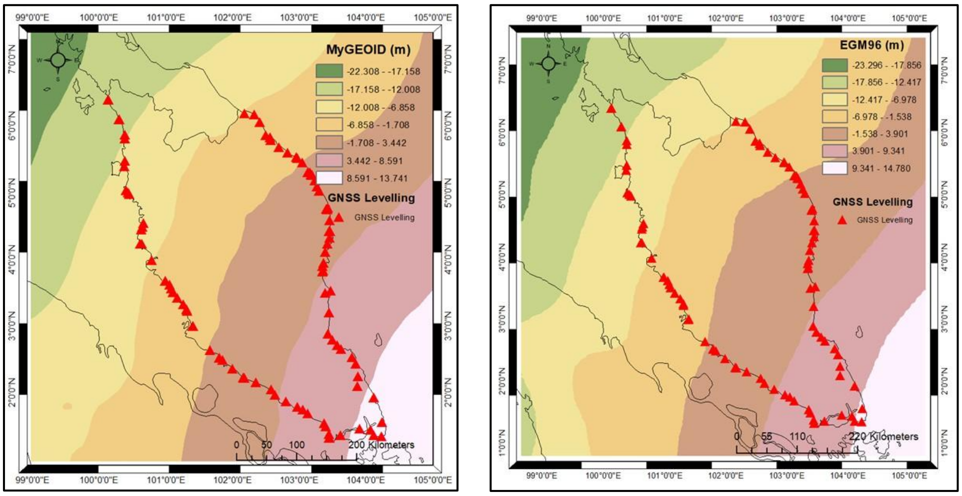

(a) (b)

Fig. 6. IDW Interpolation of Geoid Height, N, from (a) MyGEOID and (b) EGM1996 for Peninsular Malaysia

Source: Authors (2025)

Determination of Orthometric Height, H, from GNSS Levelling

The GNSS levelling data are used as a reference datum to assess the accuracy of GDEM data. Orthometric Height from GNSS Levelling. Two (2) parameters are required to determine the orthometric height, H, for the 199 GNSS levelling observation points, namely the ellipsoidal height, h, from TBC and geoid height, N, from MyGEOID. The formula for calculating the orthometric height, H, is shown in Equation 4.

$$H = h_{GNSS} - N_{MyGEOID} \tag{4}$$

where,

H: Orthometric height (Topography)
h: Ellipsoidal height from GNSS levelling
N: Geoid height (MyGEOID)

Determination of Orthometric Height for GDEM

To assess the accuracy of the GDEM, the extracted elevation from Global Mapper must be converted to local orthometric height, H, making it compatible with the orthometric height, H, from the GNSS levelling. Therefore, the extracted GDEM elevations for ASTER, ALOSW3D, and SRTM were converted to the local orthometric height, H, using both EGM1996 and MyGEOID using Equations 5 and 6. The reason why EGM1996 is used instead of only MyGEOID because the vertical datum from SRTM, ASTER, and ALOSW3D is EGM1996, meaning the extracted elevation for SRTM, ASTER and ALOSW3D from Global Mapper was referenced to EGM1996. Hence, the orthometric height for SRTM, ASTER and

https://doi.org/10.24191/bej.v23i2.8382

ALOSW3D was determined by adding the extracted elevation from Global Mapper with EGM1996, and then subtracting it from MyGEOID to make it compatible with the GNSS levelling data.

$$h_{SRTM/ASTER/ALOSW3D} = H_{SRTM/ASTER/ALOSW3D} + N_{EGM1996} \tag{5}$$

$$H_{SRTM/ASTER/ALOSW3D} = h_{SRTM/ASTER/ALOSW3D} - N_{MyGEOID} \tag{6}$$

where,

$h_{SRTM/ASTER/ALOSW3D}$: Ellipsoidal height for SRTM 30/90, ASTER, and ALOSW3D
$H_{SRTM/ASTER/ALOSW3D}$: Orthometric height, H, for SRTM 30/90, ASTER, and ALOSW3D
$N_{MyGEOID}$: Geoid height for MyGEOID
$N_{EGM1996}$: Geoid height for EGM1996

However, for the determination of orthometric height, H for TanDEM-X, there is a slight difference in the formula as stated in Equation 7. Only MyGEOID were used because the vertical datum for TanDEM-X is WGS84 ellipsoid, which is similar to the GNSS levelling data. Hence, the orthometric height, H, for TanDEM-X were determined directly by subtracting the extracted elevation from Global Mapper with MyGEOID.

$$H_{TanDEM-x} = h_{TanDEM-X} - N_{MyGEOID} \tag{7}$$

where,
$H_{TanDEM-x}$: Orthometric height for TanDEM-X, with respect to MyGEOID
= $h_{TanDEM-X}$: Ellipsoidal height with respect to WGS84 for TanDEM-X
$N_{MyGEOID}$: Geoid height from MyGEOID

RESULTS AND DISCUSSION

Comparison of Orthometric Height Between GDEM and GNSS Levelling

The statistical analysis for the comparison of orthometric height, H, between the GDEM and GNSS is illustrated in Figure 7. The statistical assessment of the GDEM with GNSS levelling is tabulated in Table 2.

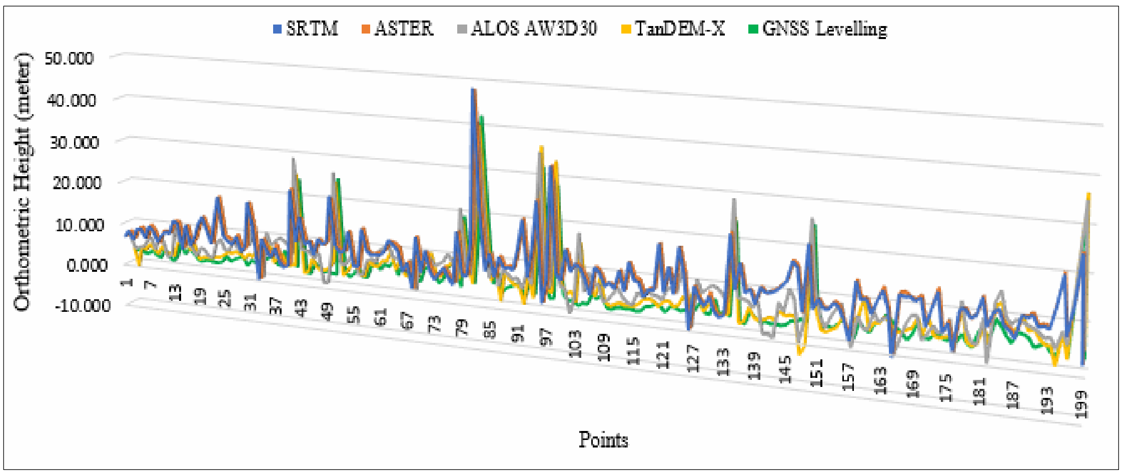

Fig. 7. Comparison of Orthometric Height, H of SRTM, ASTER, ALOSW3D and TanDEM-X with GNSS Levelling
Source: Authors (2025)

Table 2. Statistical Assessment of GDEM with GNSS Levelling

Statistical Assessment	SRTM	ASTER	ALOSW3D	TanDEM-X
Min (m)	-0.656	-0.675	-0.675	-3.742
Max (m)	49.006	48.610	41.399	40.178
Median (m)	9.676	9.772	6.679	4.568
Sum (m)	2067.020	2067.017	1549.785	1225.575
Mean (m)	10.387	10.387	7.788	6.159
Standard Deviation (m)	5.406	5.406	6.148	6.186
Standard Error (m)	0.383	0.383	0.436	0.439
Mean Absolute Error (m)	11.354	11.366	6.267	3.099
RMS (m)	10.387	10.387	7.788	6.159
RMSE (m)	3.220	3.220	2.790	2.480

Source: Authors (2025)

The statistical analysis of RMSE between the GDEM and GNSS levelling was conducted using Equation 1. From the analysis, the result depicts that SRTM and ASTER have a similar RMSE of 3.220 m. On the other hand, ALOSW3D illustrates an RMSE of 2.790 m. Last but not least, TanDEM-X exhibit the smallest RMSE of 2.480 m. As for the correlation coefficient, R analysis, the calculation was performed based on Equation 2. The correlation coefficient, R, analysis between ASTER, ALOSW3D, SRTM, and TanDEM-X, respectively, with GNSS levelling, is illustrated in Figure 8.

The correlation analysis revealed that the R values for ASTER, ALOSW3D, SRTM, and TanDEM-X were 0.513, 0.830, 0.514, and 0.899, respectively, when compared against GNSS levelling benchmarks. These results demonstrate that TanDEM-X exhibited the strongest correlation and highest accuracy, outperforming the other datasets, with an RMSE of 2.480 m and a correlation coefficient (R) of 0.900. Moreover, as for the Mean Absolute Error (MAE) results (SRTM = 11.354 m, ASTER = 11.366 m, ALOS AW3D = 6.267 m, TanDEM-X = 3.099 m), they reflect fundamental differences in sensor type, spatial resolution, and processing. TanDEM-X's interferometric SAR acquisition and global mosaicking produce substantially lower random noise and better global calibration, explaining the lowest MAE (~72.7% lower than SRTM). ALOS AW3D's higher-quality optical stereo processing yields intermediate performance (≈44.8% improvement over SRTM). SRTM and ASTER show similar, larger MAEs likely due to canopy/top-of-surface penetration (radar), stereo correlation failures, void-filling artefacts, and temporal mismatches with the GNSS levelling dataset. These MAE values should be interpreted alongside tests by landcover and slope, checks on vertical datum consistency, and assessment of GNSS reference precision to ensure the observed differences reflect DEM quality rather than sampling or datum errors.

https://doi.org/10.24191/bej.v23i2.8382

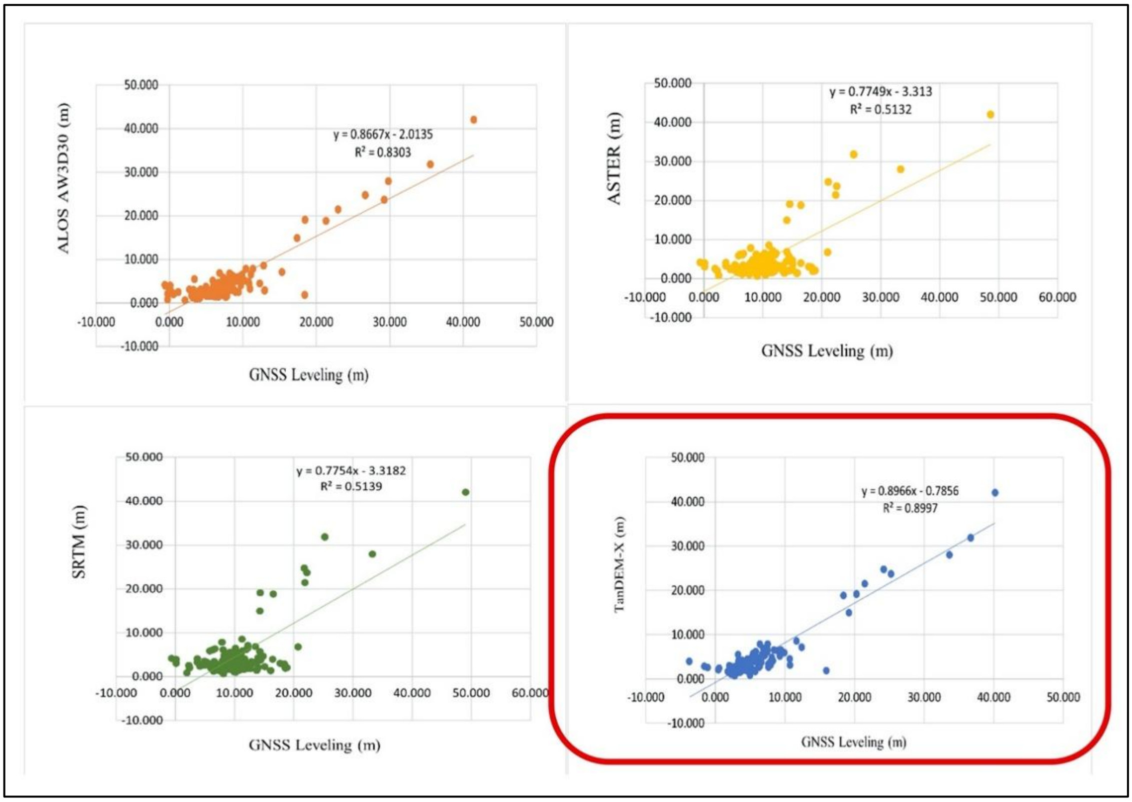

Fig. 8. Correlation Coefficient, R of ALOSW3D, ASTER, SRTM and TanDEM-X, and GNSS Levelling in The Coastal Region of Peninsular Malaysia

Source: Authors (2025)

Comparison of RMSE, Correlation Coefficient, R and MAE of GDEM with GNSS Levelling

The statistical assessment based on orthometric height, H, for the open-source DEM with the GNSS levelling observation is based on the RMSE, correlation coefficient, R and MAE (Khalid et al., 2016; Pa'suya et al., 2019; Abd Rahman et al., 2022a). The statistical assessment of RMSE and Correlation coefficient, R, for SRTM, ASTER, ALOSW3D and TanDEM-X are shown in Figure 9.

The superior performance of TanDEM-X compared to other GDEMs can be attributed to several potential factors. Firstly, while both SRTM and TanDEM-X employ Synthetic Aperture Radar (SAR) technology, ASTER and ALOSW3D rely on optical imaging systems. SRTM operates using both C-band radar, with a wavelength of 5.6 cm, and X-band radar, with a wavelength of 3.1 cm. The TerraSAR and TanDEM-X satellites use the X-band (wavelength of 3.1 cm) (Kellndorfer et al., 2019). On the other hand, ASTER and ALOSW3D use the optical imaging system with wavelengths of 0.78 to 0.86 µm and 0.52 to 0.77 µm, respectively (Kellndorfer et al., 2019). The difference between SAR and optical imaging technology is that SAR operates using radiowaves, which carry their illumination in radiowaves form transmitted by the antenna (Kellndorfer et al., 2019). On the contrary, optical imaging works using an optical sensor, which relies on illumination from the sun and thermal radiation to create the brightness for observation by the sensor (Kellndorfer et al., 2019).

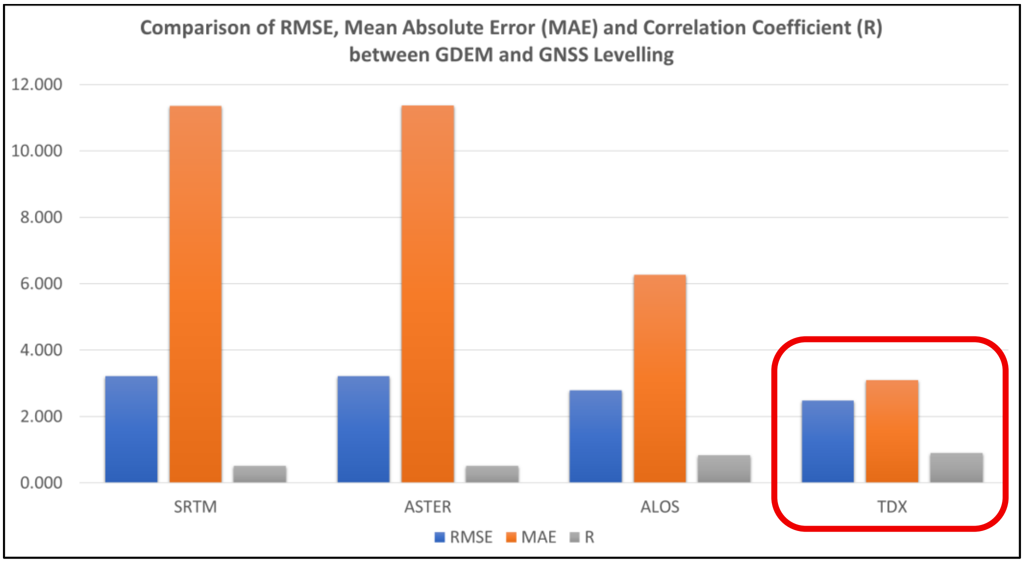

Fig. 9. Overall Evaluation of the SRTM, ASTER, ALOSW3D, and TanDEM-X with GNSS Levelling

Source: Authors (2025)

According to Liu et al. (2018), when dealing with SAR, the wavelength is a crucial factor to take into account since it affects how the radar signal interacts with the surface and how far a signal may travel through a medium. A radar signal with a longer wavelength travel further than a shorter wavelength due to its lower frequency (Singh et al., 2021a). Furthermore, the radar signal with a longer wavelength used by TanDEM-X and SRTM in this study is capable of penetrating the clouds, which results in a more accurate depiction of the Earth's topography (Singh et al., 2021b). On the other hand, the signal with a short wavelength used by ASTER and ALOSW3D, for example, might be obstructed or reflected by similar obstacles (Singh et al., 2021a). Therefore, such a reason explains why utilising SAR (SRTM and TanDEM-X) for data acquisition outperformed the utilisation of optical imaging systems in ASTER and ALOSW3D, as illustrated in this study (Singh et al., 2021a; Singh et al., 2021b; Grohman, 2018)

According to Vassilaki & Stamos (2020) and El-Ashmawy (2024), the other reason TanDEM-X is superior in comparison to the other open-source DEMs is due to the utilisation of TerraSAR-X (starting in 2007) and TanDEM-X (starting in 2010), the two (2) SAR satellites that fly in a close orbit configuration at an altitude of 514 km, and each satellite operates using the X-band single-pass interferometer (Hussaini et al., 2024). TanDEM-X and TerraSAR-X operate as a dual-satellite system for data acquisition, maintaining a typical cross-track separation of 300 to 500 meters. This configuration enables a flexible single-pass SAR interferometry setup, supporting both across-track and along-track interferometry during data collection. In contrast, other GDEMs such as SRTM, ASTER, GMTED, and ALOSW3D rely on a single-satellite system for their data acquisition processes (Adiri et al., 2022; Tabunshchik et al., 2023; Yogi & Stanganini, 2023)

Moreover, regarding the analysis of error patterns, even though TanDEM-X performed quite well in general, there were large outliers across all datasets, with maximum deviations on the order of approximately 40.000-50.000 m, in particular in SRTM and ASTER. These large errors may be related to multiple overlapping causes such as vegetation canopy interference (optical sensors such as ASTER and ALOSW3D record the top of the canopy rather than the ground), discrepancies in radar signal penetration

(SRTM's C-band can partially penetrate vegetation cover and wet surfaces, whereas TanDEM-X's X-band can provide better structural detail but is more sensitive to surface roughness), complexity of coastal terrain (particularly in mangrove swamps, tidal marshes, estuarine deltas, and previous urban areas) that known to cause heterogeneous backscatter and shadowing, and GNSS benchmark placement (some levelling points were further inland, away from the coast which leads to slight elevation differences). The main findings here indicate that terrain type and surface characteristics exert more influence on DEM accuracy than sensor resolution alone. Thus, the potential directions for future work could include bias corrections or outlier filtering to further evaluate the impact of these extreme values on the overall RMSE performance

In addition, with regard to the spatial variability of accuracy, the statistical results provide average statistics that are descriptive of the overall accuracy, but the accuracy of the DEM does not vary consistently along the Malaysian coastline. At a larger scale, the larger discrepancies occurred at the delta locations along the west coast, chiefly in Klang, Perak, and Selangor, where dense mangroves and reclaimed industrial sites interfered with radar backscatter and optical reflectance. In comparison, the flatter east coastal areas, such as Kelantan and Terengganu, had much smaller residuals and lower dispersion in error, due to lower vegetation cover and less rugged terrain. However, the greater elevation gradient or gradient in the coastal slope is likely not the cause of increased vegetation structure and surface roughness. Therefore, where mapping of the residuals occurred spatially, a zone of terrain-dependent performance could be identified that would help narrow down the selection of an appropriate DEM for local use for the separate sites on the east and west coasts. More recently, El-Ashmawy (2024) and Hussaini et al. (2024) have supported consensus in that SAR-based DEMs perform better in humid, vegetated regions than those of optical systems

Despite being numerically small (between 0.700 and 1.000 m between TanDEM-X and SRTM/ASTER), the observed RMSE differences are extremely significant for flood-risk modelling. Even a 1-meter elevation difference can determine whether land is considered safe or inundated under sea-level-rise scenarios in low-lying deltaic environments. A 1-meter underestimation of elevation, for example, could result in an underestimation of flood extent by several square kilometres in regions like the Kota Bharu floodplain or the Klang Delta. TanDEM-X can therefore significantly lower the risk of misclassification and improve model reliability in disaster preparedness and coastal management planning when used in coastal erosion and inundation studies. While this study offers valuable insights into the vertical accuracy of four (4) major GDEMs, several limitations should be noted. First, the analysis mainly focuses on coastal benchmarks and does not include inland highlands that may show different error patterns. Second, the evaluation primarily used RMSE and correlation metrics, which assess overall accuracy but do not account for systematic bias or spatial error trends. Future research should include bias analysis, assessments based on different terrains, and cross-validation with LiDAR, Copernicus DEM, or ICESat-2 data. Researchers should also consider using machine learning methods to correct systematic elevation errors and improve the vertical precision of global DEMs in tropical areas.

CONCLUSION

This study aimed to evaluate the accuracy of four (4) GDEMs—SRTM, ASTER, ALOSW3D, and TanDEM-X—using 199 GNSS fast-static levelling observations as the reference dataset. Statistical analysis based on RMSE revealed values of 3.220 m for both SRTM and ASTER, 2.790 m for ALOSW3D, and 2.480 m for TanDEM-X. The correlation coefficient (R) analysis showed R-values of 0.514 for SRTM, 0.513 for ASTER, 0.830 for ALOSW3D, and 0.900 for TanDEM-X. Similarly, TanDEM-X also exhibit the best MAE of 3.099m in comparison to SRTM (11.354 m), ASTER (11.366 m) and ALOSW3D (6.267 m). These results indicate that TanDEM-X exhibits the highest accuracy among the four (4) models, with the lowest RMSE and the strongest correlation with the GNSS reference data. The superior performance of

TanDEM-X can be attributed to its use of Synthetic Aperture Radar (SAR), which does not rely on solar illumination or thermal radiation like optical sensors.

Furthermore, TanDEM-X benefits from its dual-satellite system, TanDEM-X (2010) and TerraSAR-X (2007), which operate in close orbital formation with a typical cross-track separation of 300 to 500 meters. This configuration enables both across-track and along-track interferometry during data acquisition, unlike the single-satellite systems used by the other GDEMs. In addition, outliers of up to 50 m were mainly found along vegetated and reclaimed west coast areas, while the flatter east coast showed smaller residuals, highlighting the influence of surface roughness and land cover on DEM accuracy. Although numerically small, these elevation differences have critical implications for flood-risk and coastal modelling, where a 1 m bias may alter inundation classifications. Overall, TanDEM-X is the most reliable GDEM for coastal applications in Malaysia. Future studies should extend validation to inland terrains and explore LiDAR or ICESat-2 comparisons for further refinement.

ACKNOWLEDGEMENTS/FUNDING

The authors would like to thank the Department of Surveying and Mapping Malaysia (DSMM) for providing the MyGEOID data for this study. The authors are also indebted to JAXA, Earth data, Geoservices, NASA, and ICGEM for providing the GDEM (SRTM, ASTER, ALOSW3D and TanDEM-X) and EGM1996 data for free. The authors would also like to thank Universiti Geomatika Malaysia (UGM) for funding this research under the Research, Innovation and Commercialisation Centre (RICC).

CONFLICT OF INTEREST STATEMENT

The authors agree that this research was conducted in the absence of any self-benefits, commercial or financial conflicts and declare the absence of conflicting interests with the funders.

AUTHORS' CONTRIBUTIONS

Mohd Faizuddin Abd Rahman and Siti Nurshahira Yamen carried out the data acquisition, processing, analysis and discussion. Ami Hassan, Md Din assisted in assessing the results of the analysis and discussion. He also contributed to improving the literature review for this study.

REFERENCES

Abd Rahman, M. F., Din, A. H. M., Abd Hamid, A. I., Alihan, N. S. A., Yazid, N. M., Ansar, A. M. H., & Junid, M. A. H. (2022a). Accuracy Assessment of Open-source Global Digital Elevation Models (DEM) With Global Navigation Satellite System (GNSS) Levelling. In IOP Conference Series: Earth and Environmental Science (Vol. 1064, No. 1, p. 012018). IOP Publishing, https://doi.org/10.1088/1755-1315/1064/1/012018

Adiri, Z., Lhissou, R., Maacha, L., Jilali, A., Talbi, E. H., Jellouli, A., & Chakouri, M. (2022). Comparison of ASTER GDEM3, SRTM3, NASADEM, TanDEM-X90, AW3D30, and ALOS PALSAR data with TanDEM-X12: A case study of Tagragra of Akka inlier, Moroccan Anti-Atlas. *Arabian Journal of Geosciences*, *15*(21), 1654. https://doi.org/10.48346/IMIST.PRSM/ajlp-gs.v7i4.49875

Albayrak, M., Özlüdemir, M. T., Aref, M. M., & Halicioglu, K. (2020). Determination Of Istanbul Geoid Using GNSS/Levelling and Valley Cross Levelling Data. *Geodesy and Geodynamics*, 11(3), 163-173, https://doi.org/10.1016/j.geog.2020.01.003

Athmania, D., & Achour, H. (2014). External validation of the ASTER 2, GMTED2010, and CGIAR-CSI-SRTM v4.1 free access digital elevation model (DEMs) in Tunisia and Algeria. *Remote Sensing*, 6(5), 4600–4620 https://doi.org/10.3390/rs6054600

Chai, T., & Draxler, R. R. (2014). Root Mean Square Error (RMSE) Or Mean Absolute Error (MAE). Geoscientific Model Development Discussions, 7(1), 1525-1534, https://doi.org/10.5194/gmdd-7-1525-2014

Du, X., Guo, H., Fan, X., Zhu, J., Yan, Z., & Zhan, Q. (2012). Vertical accuracy assessment of SRTM and ASTER over coastal regions of China: A comparative analysis. 33rd Asian Conference on Remote Sensing 2012, ACRS 2012, 2, 1236–1243. https://api.semanticscholar.org/CorpusID:132651871

El-Ashmawy, K. L. (2024). Vertical Accuracy of Google Earth Data. Engineering, Technology & Applied Science Research, 14(3), 13830-13836. https://doi.org/10.48084/etasr.7121

Fazilah, S. R. (2006). An Assessment of GPS Heighting from MyRTKnet and MyGEOID Compared to Conventional Levelling, Undergraduate thesis, Universiti Teknologi Petronas, Malaysia. http://utpedia.utp.edu.my/id/eprint/7815

Glen, S. (2020a). RMSE: Root Mean Square Error. RMSE from StatisticsHowTo.com: Elementary Statistics for the rest of us! https://www.statisticshowto.com/probability-and-statistics/correlation-coefficient-formula/

Glen, S. (2020b). Correlation Coefficient: Simple Definition, Formula, Easy Steps. from StatisticsHowTo.com: Elementary Statistics for the rest of us! https://www.statisticshowto.com/probability-and-statistics/correlation-coefficient-formula/

Gogtay, N. J., & Thatte, U. M. (2017). Principles Of Correlation Analysis. Statistics for Researcher: Principles of Correlation Analysis. *Journal of the Association of Physicians of India*, 65(3), 78-81. https://pubmed.ncbi.nlm.nih.gov/28462548/

Gorokhovich, Y., & Voustianiouk, A. (2006). Accuracy assessment of the processed SRTM-based elevation data by CGIAR using field data from the USA and Thailand, and its relation to the terrain characteristics. *Remote Sensing of Environment*, 104(4), 409–415. https://doi.org/10.1016/j.rse.2006.05.012

Grohman, C. H. (2018). Evaluation of TanDEM-X DEMs on Selected Brazilian Sites: Comparison with SRTM, ASTER GDEM and ALOS AW3D30. *Remote Sensing of Environment*, 212, 121-133. https://doi.org/10.1016/j.rse.2018.04.043

Halim, S. M. A., Green, M. F. P. S., Narashid, R. H., & Din, A. H. M. (2019). Accuracy Assessment of TanDEM-X 90 m Digital Elevation Model in East of Malaysia Using GNSS/Levelling. ICSGRC 2019 - 2019 IEEE 10th Control and System Graduate Research Colloquium, Proceedings, 88–93 https://doi.org//10.1109/ICSGRC.2019.8837059

Hussaini, A., Wee, K. T. K., Hamid, A. I. A., Abubakar, A. G., & Tan, C. W. (2024). Comparative Analysis of GDM2000, WGS84, and MRT68 Coordinate Reference Systems based on Different Converter Modules. *Engineering, Technology & Applied Science Research*, 14(4), 15494-15498. https://doi.org/10.48084/etasr.7124

Ismail, M. K., Din, A. H. M., Uti, M. N., & Omar, A. H. (2018). Establishment Of New Fitted Geoid Model In Universiti Teknologi Malaysia. The International Archives of Photogrammetry, Remote Sensing and Spatial Information Sciences, 42, 27-33, https://doi.org/10.5194/isprs-archives-XLII-4-W9-27-2018

Kellndorfer, J., Flores-Anderson, A. I., Herndon, K. E., & Thapa, R. B. (2019). Using SAR Data for Mapping Deforestation and Forest Degradation. The SAR Handbook. Comprehensive Methodologies for Forest Monitoring and Biomass Estimation; ServirGlobal: Huntsville, AL, USA, 65-79. https://doi.org/10.25966/68c9-gw82

Khalid, N. F., Din, A. H. M., Omar, K. M., Khanan, M. F. A., Omar, A. H., Hamid, A. I. A., & Pa'Suya, M. F. (2016). Open-source digital elevation model (DEM) evaluation with GPS and lidar data. International Archives of the Photogrammetry, Remote Sensing and Spatial Information Sciences - ISPRS Archives, 42(4W1), 299–306 https://doi.org/10.5194/isprs-archives-XLII-4-W1-299-2016

Kumar, N., & Jha, R. (2023). GIS-based flood risk mapping: The case study of Kosi River Basin, Bihar, India. *Engineering, Technology & Applied Science Research*, 13(1), 9830-9836. https://doi.org/10.48084/etasr.5377

Lemoine, F. G., Kenyon, S. C., Factor, J. K., Trimmer, R. G., Pavlis, N. K., Chinn, D. S., ... & Olson, T. R. (1998). The Development of the Joint NASA GSFC and the National Imagery and Mapping Agency (NIMA) Geopotential Model EGM1996 (No. NAS 1.60: 206861). chrome-extension://efaidnbmnnnibpcajpcglclefindmkaj/https://ntrs.nasa.gov/api/citations/19980218814/downloads/19980218814.pdf

Leon, J. X., Heuvelink, G. B. M., & Phinn, S. R. (2014). Incorporating DEM uncertainty in coastal inundation mapping. PLoS ONE, 9(9), 1–12. http://doi.org/10.1371/journal.pone.0108727

Liu, C., Chen, J., Liu, T., Heimbach, F., Yu, H., Xiao, Y., & Wu, M. (2018). Long-Distance Propagation of Short-Wavelength Spin Waves. *Nature communications*, 9(1), 738. https://doi.org/10.1038/s41467-018-03199-8

Mukherjee, S., Joshi, P. K., Mukherjee, S., Ghosh, A., Garg, R. D., & Mukhopadhyay, A. (2012). Evaluation of vertical accuracy of open-source Digital Elevation Model (DEM). *International Journal of Applied Earth Observation and Geoinformation*, 21(1), 205–217. https://doi.org/10.1016/j.jag.2012.09.004

Nordin, A. F., Abu, S. H. J., Hua Ch, L., & Nordin, S. (2005, September). Malaysia Precise Geoid (MyGEOID). Coordinates, 1(4), 30-37. (Accessed on https://mycoordinates.org/malaysia-precise-geoid-mygeoid/all/1/#:~:text=The%20Malaysian%20geoid%20project%20(MyGEOID,for%20cadastral%20and%20mapping%20purposes)

Pa'suya, Muhammad Faiz, Din, A. H. M., Amin, Z. M., Omar, K. M., Omar, A. H., & Rusli@Ruslik, N.

(2019). Evaluation of Global Digital Elevation Model for Flood Risk Management in Perlis. In Lecture Notes in Civil Engineering (Vol. 9, pp. 1007–1017). Springer. https://doi.org/10.1007/978-981-10-8016-6_70

Rao, B. S., Kumar, G. A., Srinivasulu, P., & Venkataraman, V. R. (2012). Evaluation Of EGM 2008 With EGM1996 And Its Utilisation in Topographical Mapping Projects. Journal of the Indian Society of Remote Sensing, 2(40), 335-340, https://doi.org/10.1007/s12524-011-0131-1

Singh, P., Diwakar, M., Shankar, A., Shree, R., & Kumar, M. (2021a). A Review on SAR Image and Its Despeckling. Archives of Computational Methods in Engineering, 28, 4633-4653. https://doi.org/10.1007/s11831-021-09548-z

Singh, P., Shree, R., & Diwakar, M. (2021b). A New SAR Image Despeckling Using Correlation-Based Fusion and Method Noise Thresholding. *Journal of King Saud University* - Computer and Information Sciences, 33(3), 313-328. https://doi.org/10.1016/j.jksuci.2018.03.009

Tabunshchik, V., Gorbunov, R., Gorbunova, T., Pham, C. N., & Klyuchkina, A. (2023). Identification of river basins within northwestern slope of Crimean Mountains using various digital elevation models (ASTER GDEM, ALOS World 3D, Copernicus DEM, and SRTM DEM). *Frontiers in Earth Science*, *11*, 1218823. https://doi.org/10.3389/feart.2023.1218823

Van de Sande, B., Lansen, J., & Hoyng, C. (2012). Sensitivity of Coastal Flood Risk Assessments to Digital Elevation Models. Water, 4(3), 568–579. http://doi.org/10.3390/w4030

Vassilaki, D. I., & Stamos, A. A. (2020). TanDEM-X DEM: Comparative Performance Review Employing LiDAR Data And DSM. *ISPRS Journal of Photogrammetry and Remote Sensing*, 160, 33-50. https://doi.org/10.1016/j.isprsjprs.2019.11.015

Yogi, F., & Stanganini, F. N. (2023). Comparação e Avaliação de Modelos Digitais de Elevação dos sensores SRTM, ASTER, TANDEM/TERRASAR–X, NASADEM, COPERNICUS DEM e ALOS PALSAR para análise digital de terreno para aplicações no saneamento básico. *Research, Society and Development*, *12*(1), e13812139350-e13812139350. https://doi.org/10.33448/rsd-v12i1.39350